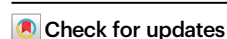


Brain age prediction and deviations from normative trajectories in the neonatal connectome

Received: 15 May 2024

Accepted: 13 November 2024

Published online: 26 November 2024

Huili Sun¹✉, Saloni Mehta², Milana Khaitova², Bin Cheng³, Xuejun Hao⁴, Marisa Spann^{4,5} & Dustin Scheinost^{1,2,6,7,8}

Structural and functional connectomes undergo rapid changes during the third trimester and the first month of postnatal life. Despite progress, our understanding of the developmental trajectories of the connectome in the perinatal period remains incomplete. Brain age prediction uses machine learning to estimate the brain's maturity relative to normative data. The difference between the individual's predicted and chronological age—or brain age gap (BAG)—represents the deviation from these normative trajectories. Here, we assess brain age prediction and BAGs using structural and functional connectomes for infants in the first month of life. We use resting-state fMRI and DTI data from 611 infants (174 preterm; 437 term) from the Developing Human Connectome Project (dHCP) and connectome-based predictive modeling to predict postmenstrual age (PMA). Structural and functional connectomes accurately predict PMA for term and preterm infants. Predicted ages from each modality are correlated. At the network level, nearly all canonical brain networks—even putatively later developing ones—generate accurate PMA prediction. Additionally, BAGs are associated with perinatal exposures and toddler behavioral outcomes. Overall, our results underscore the importance of normative modeling and deviations from these models during the perinatal period.

The human connectome—a whole-brain connectivity map—undergoes rapid changes during the perinatal period. The structural connectome is established across the third trimester¹. For example, hallmark topological properties of the structural connectome, including rich-club connections², network controllability³, and connectome fingerprinting⁴, are observable at birth. Structural connections mature further during the first year of life but slow down afterward⁵. In contrast, the functional connectome develops slower in the fetal period. Early functional connections are

observed in the fetal period⁶, and lower-order networks (e.g., motor-sensory) are present at birth⁵. However, many functional networks (e.g., the default mode network) only resemble older children after the first year of life^{7,8}. Nevertheless, emerging research suggests that most functional networks are detectable in the neonatal period⁹ with larger samples and higher-quality data. Thus, despite progress in mapping developmental trajectories in the perinatal period, a normative model of the early connectome does not exist.

¹Department of Biomedical Engineering, Yale University, New Haven, CT, USA. ²Department of Radiology & Biomedical Imaging, Yale School of Medicine, New Haven, CT, USA. ³Department of Biostatistics, Mailman School of Public Health, Columbia University, New York, NY, USA. ⁴New York State Psychiatric Institute, New York, NY, USA. ⁵Department of Psychiatry, Vagelos College of Physicians and Surgeons, Columbia University, New York, NY, USA. ⁶Department of Statistics & Data Science, Yale University, New Haven, CT, USA. ⁷Child Study Center, Yale School of Medicine, New Haven, CT, USA. ⁸Wu Tsai Institute, Yale University, New Haven, CT, USA. ✉e-mail: huili.sun@yale.edu

Brain age prediction is a novel approach to normative modeling^{10,11}. This approach consists of two steps. First, a machine learning model is trained to predict an individual's age using neuroimaging data, where the predicted results reflect the individual brain maturation level compared to the whole group. Predicted ages for different brain regions can be compared to investigate correlational patterns of developmental trajectories across the brain networks. Second, the difference between the individual's predicted and chronological age—or brain age gap (BAG)—is calculated. BAGs represent the deviation from normative brain measures at any particular age. Other participant characteristics (e.g., behavior or disease symptoms) can be associated with BAGs to investigate their impact on normative development or aging. While research using brain age predictions and BAGs is robust in adolescents and adults^{12,13}, fewer studies of BAGs with connectome data from the perinatal period exist. Four studies^{9,14–16} have used functional connectomes, and five^{17–21} have used structural connectomes to predict age in the first months of life. However, none of these studies have compared structural and functional brain ages.

Early life exposures and later toddler behavior are important phenotypes to investigate with normative developmental models, like BAGs. Numerous perinatal exposures, including maternal mental health^{22–25}, physical health^{26–28}, and substance use^{29,30}, contribute to individual differences in neurodevelopmental trajectories. These exposures push and pull development to better or worse trajectories. Likewise, early deviations from a normative model may reflect future risk of disorders. Therefore, BAGs during the perinatal period might eventually help with risk identification. Previous studies have not correlated BAGs with early life exposures. Further, only one correlated BAGs with later toddler behavior in preterm infants¹⁷.

Here, we assess brain age prediction and BAGs of structural and functional connectomes for infants in the first month of life. We asked the following questions: How do structural and functional connectomes mature during the perinatal period? How correlated is structural and functional development at this age? How do individual canonical brain networks mature in distinctive patterns after birth?

How do perinatal maternal exposures alter normative development (e.g., BAGs)? How do BAGs in infants predict toddler cognition and behavior? To answer these questions (Fig. 1), we calculated brain age and BAGs based on resting-state fMRI and DTI for 611 infants (174 preterms; 437 terms) from the Developing Human Connectome Project³¹ (dHCP, <http://www.developingconnectome.org/>) using connectome-based predictive modeling (CPM). Both structural and functional connectomes accurately predicted postmenstrual age (PMA) for preterm and term infants. Predicted PMA from structural and functional connectomes were correlated. Several canonical brain networks predicted PMA. Multiple prenatal maternal effects altered BAGs in the two groups, and BAGs were associated with development outcomes in toddlerhood. Together, we established normative models of connectome development in infants and highlighted that deviations associate with early-life maternal exposures and later behavior.

Results

We used multimodal neuroimaging data for 611 infants (174 preterms; 437 terms) from the developing Human Connectome Project (dHCP). Term infants were born between 37.00 and 42.29 weeks of gestation and scanned between 37.43 and 44.71 weeks. Preterm infants were born between 23.00 and 36.86 weeks of gestation and scanned between 26.71 and 45.14 weeks. Demographic information about the infants is presented in Table 1. Functional connectomes were created from resting-state functional magnetic resonance imaging (fMRI) data. Structural connectomes were created from diffusion weighted imaging (DWI) data. We predict postmenstrual ages (PMA) using connectome-based predictive modeling (CPM) with 10-fold cross-validation. All models controlled for sex, brain volume, and head motion. Separate models were built from the functional and structural connectomes for the term and preterm infants. Since preterm and term infants exhibit widespread differences in functional and structural connectivity^{32,33}, models were created for each group independently. Results were replicated using an additional machine learning method (support vector regression (SVR)) and shown in the Supplement (Tables S1–4).

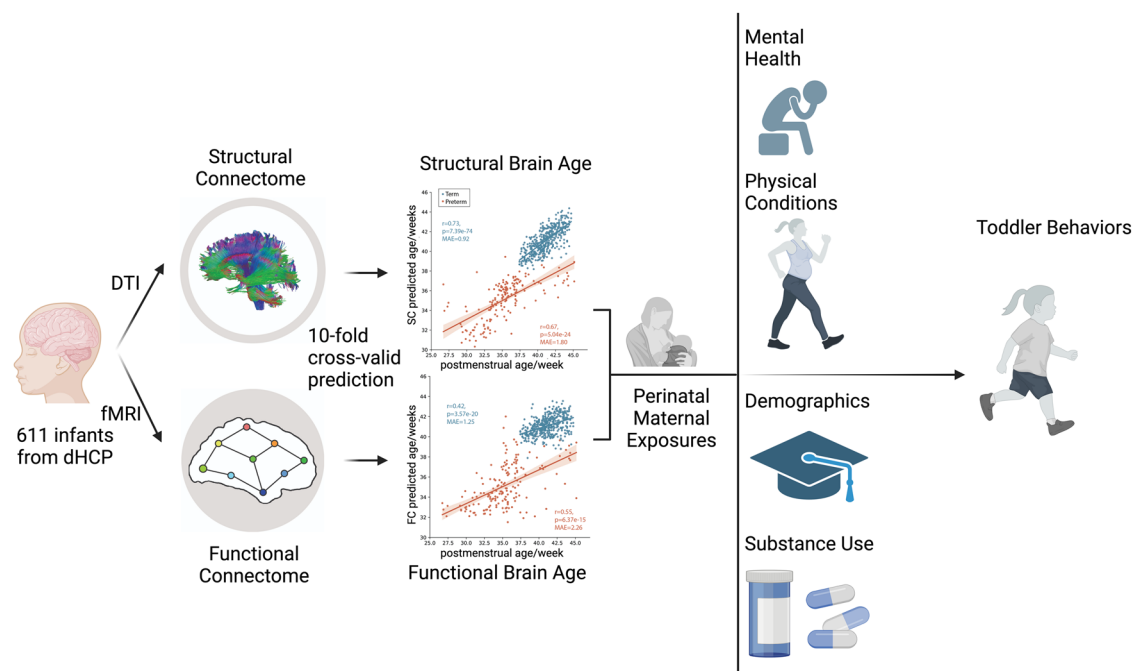


Fig. 1 | Overview of study design. Predictive models for infants' postmenstrual ages were built using structural and functional connectomes separately for term and preterm infants. Brain age gaps (BAGs) were calculated as the difference

between predicted and actual postmenstrual age. Structural and functional BAGs were associated with perinatal effects and later cognitive behaviors. Image was created in BioRender. Sun, H. (2024) [BioRender.com/m43x607](https://www.biorender.com/m43x607).

Table 1 | Infant characteristics, mean (std)

| | preterm (n = 174) | term (n = 437) | p Value |
|--|----------------------|-------------------|---------|
| Sex, num of females (%) | 74 (43.53%) | 203 (46.45%) | 0.38 |
| Gestational Age (GA) / weeks | 31.95 (3.72) | 39.90 (1.27) | |
| Post Menstrual Age (PMA) / weeks | 35.36 (3.58) | 41.14 (1.72) | |
| Bayley Scales Of Infant and Toddler Development (BSID) | n = 129 | n = 345 | |
| Cognition | 9.74 (2.53) | 10.11 (2.09) | 0.10 |
| Language | 18.44 (5.80) | 19.26 (5.09) | 0.13 |
| Motor | 19.67 (3.71) | 20.62 (3.16) | 0.0054 |
| Child Behavior Checklist (CBCL) | n = 125 | n = 337 | |
| internalizing | 45.62 (10.55) | 44.41 (9.61) | 0.24 |
| externalizing | 48.54 (9.50) | 47.53 (9.23) | 0.30 |
| total | 47.90 (9.86) | 46.91 (9.22) | 0.32 |
| Early Childhood Behavior Questionnaire (ECBQ) | n = 124 | n = 338 | |
| surgey | 5.25 (0/90) | 5.20 (0.73) | 0.56 |
| negative affect | 2.58 (0.78) | 2.63 (0.67) | 0.46 |
| effort control | 4.59 (0.69) | 4.53 (0.71) | 0.54 |
| Quantitative Checklist for Autism in Toddlers (Q-CHAT) | n = 125 | n = 338 | |
| total | 30.48 (10.30) | 30.08 (8.82) | 0.68 |

p values generated from two-sample two-sided t-tests for each row

Structural and functional connectome predict postmenstrual age in infants

Using structural connectomes, we significantly predicted PMA for term ($r = 0.73$, $p = 7.39 \times 10^{-74}$; mean absolute error (MAE) = 0.92 weeks) and preterm infants ($r = 0.67$, $p = 5.04 \times 10^{-24}$; MAE = 1.80; Fig. 2a). Similarly, using functional connectomes, we significantly predicted PMA for term ($r = 0.42$, $p = 3.57 \times 10^{-20}$; MAE = 1.25) and preterm infants ($r = 0.55$, $p = 6.37 \times 10^{-15}$; MAE = 2.26; Fig. 2b). The models trained with term infants significantly predict preterm infants' PMA and vice versa (Fig. S1). Models from structural connectomes were more accurate than models from functional connectomes (z-test, one-tail; term: $z = 7.96$, $p = 4.32 \times 10^{-14}$; preterm: $z = 2.16$, $p = 0.03$), suggesting a larger association between structural development and PMA during early infancy. Predicted ages from the structural connectomes (i.e., structural age) significantly correlated with those from the functional connectomes (i.e., functional age; term: $r = 0.36$, $p = 4.11 \times 10^{-15}$; preterm: $r = 0.50$, $p = 2.32 \times 10^{-12}$). This correlation was stronger in the preterm infants than in term infants ($z = -1.91$, $p = 0.028$). Finally, BAGs from the structural connectomes significantly correlated with BAGs from the functional connectomes for preterm ($r = 0.22$, $p = 0.0044$) but not term infants ($r = 0.092$, $p = 0.054$) when controlling for PMA.

The structural models' positive features (i.e., edges) were similar between term and preterm infants, except for connections in limbic networks. Edges within the visual network contribute the most in both groups. However, while negative features were widespread across the whole brain for term infants, fewer negative features were involved in

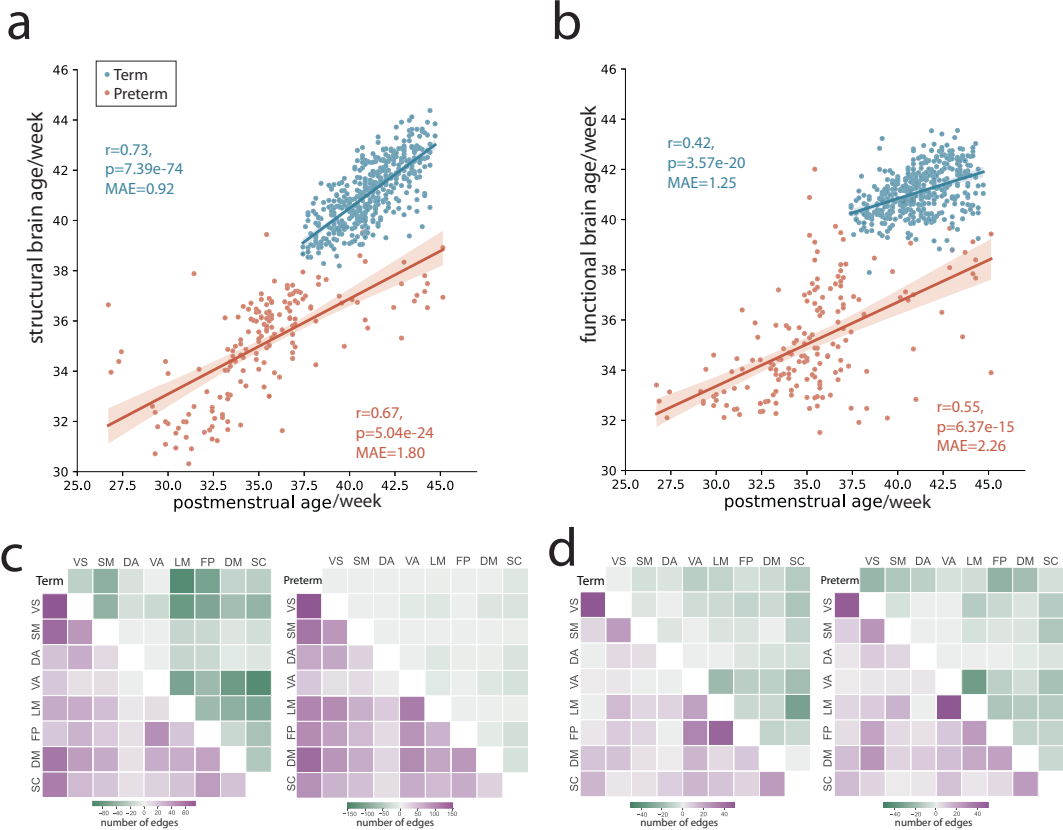


Fig. 2 | Structural and functional connectomes predict postmenstrual age (PMA) in term and preterm infants. **a** PMA was accurately predicted using structural connectomes for term (blue dots, Pearson's correlation: $r = 0.73$, $p = 7.39 \times 10^{-74}$; two-sided) and preterm infants (red dots, Pearson's correlation: $r = 0.67$, $p = 5.04 \times 10^{-24}$; two-sided). **b** PMA was accurately predicted using function connectomes for term (Pearson's correlation: $r = 0.42$, $p = 3.57 \times 10^{-20}$; two-sided) and preterm infants (Pearson's correlation: $r = 0.55$, $p = 6.37 \times 10^{-15}$; two-sided). Structural

(c) and functional (d) connections predicting term and preterm infants' PMAs. Each heatmap shows the number of edges between each pair of canonical networks during feature selection that were positively (purple) or negatively (green) correlated with postmenstrual age. VS visual, SM somatomotor, DA dorsal attention, VA ventral attention, LM limbic, FP frontoparietal, DM default mode, SC subcortical. Source data are provided as a Source Data file.

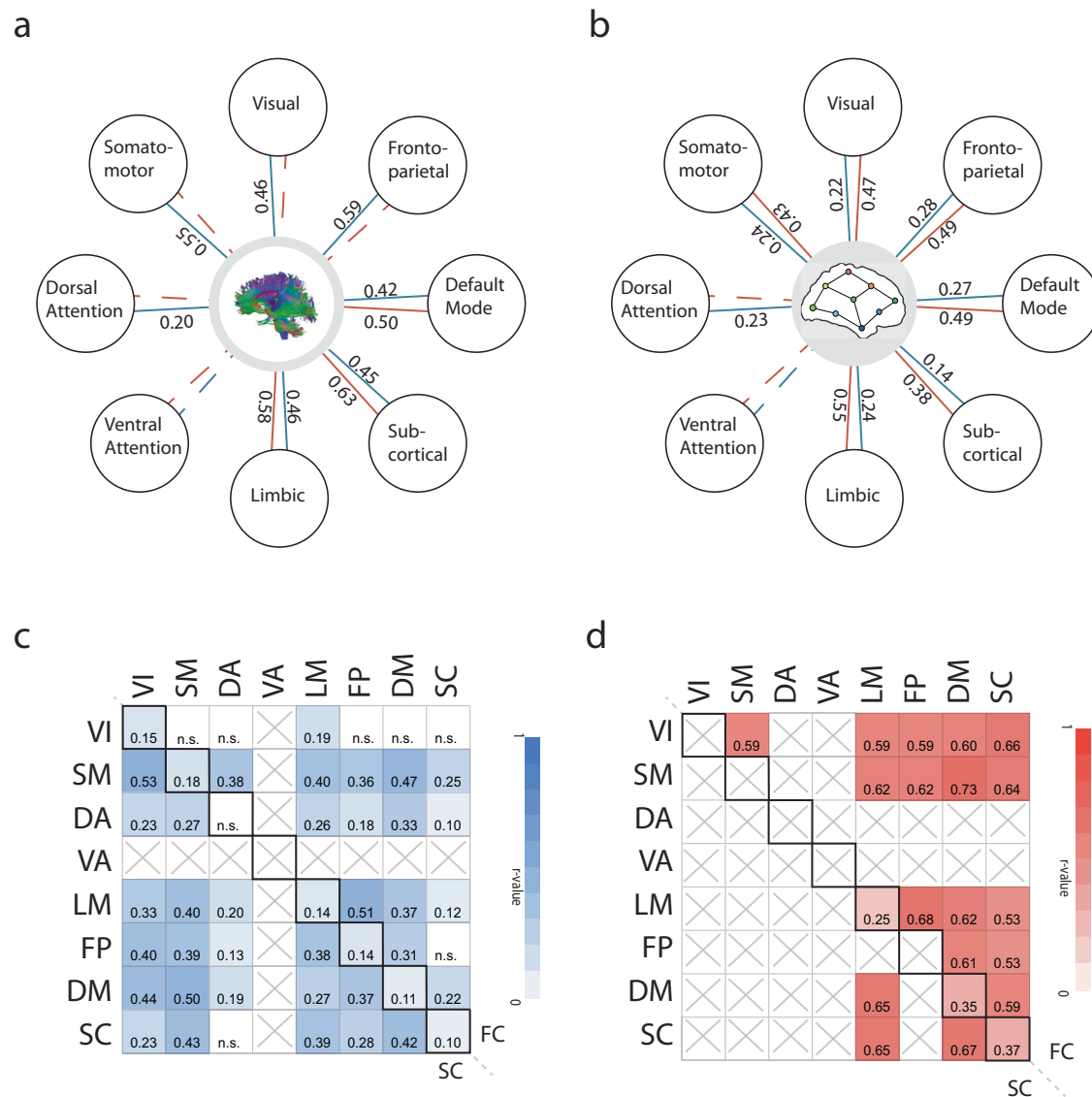


Fig. 3 | Brain network age prediction. **a** Structure and **(b)** Function canonical brain networks age predictions. Within-network connections for multiple networks successfully predicted postmenstrual age in term (blue lines) and preterm (red line) infants. Solid lines indicate significant two-sided Pearson's correlation at $p < 0.05$, FDR-corrected, while dashed lines indicate non-significant predictions. Correlations between predicted ages based on within-network connections for term **(c)** and preterm **(d)** infants. Heatmaps show the correlation between predicted PMA from within-network connections. The upper triangle shows the correlation

between functional ages. The lower triangle shows correlations between structural ages. The diagonal shows the correlations between structural and functional age for a network ($p < 0.05$; Pearson's correlation, two-sided; n.s. not significant, box crossed: age not predictable from the within-network connections). VI visual, SM somatomotor, DA dorsal attention, VA ventral attention, LM limbic, FP frontoparietal, DM default mode, SC subcortical. Source data are provided as a Source Data file.

age prediction for preterm infants. These results may indicate different development patterns in structural networks between term and preterm groups (Fig. 2c). For the functional models, the positive and negative features were similar between term and preterm infants. Positive features within the visual and frontoparietal networks significantly predicted the term infant's PMAs. Positive features within the visual and limbic network were most involved in predicting preterm infants' age. Negative features in the limbic network were involved most in the age prediction for both groups (Fig. 2d).

Structural and functional brain age for canonical networks

We investigated how connections within and between canonical brain networks predicted PMA to provide PMA prediction at greater spatial specificity. Connectomes were divided into eight canonical brain networks: visual, somatomotor, frontoparietal, default mode, dorsal

attention, ventral attention, limbic, and subcortical networks³⁴ (Table S5). For each network, the predicted age was generated based only on the connections within this network (i.e., connections between nodes in the same network). For structural and functional connectomes, all but the ventral attention network predicted PMA for term infants. In both cases, the frontoparietal network showed the highest correlation between predicted and observed PMA (structure: $r = 0.59$, $p = 6.05 \times 10^{-43}$, MAE = 1.12 weeks; Fig. 3a; function: $r = 0.28$, $p = 1.41 \times 10^{-9}$, MAE = 1.41 weeks; Fig. 3b). Like the whole-brain models, structure better predicted PMA than function in all networks (z 's > 2.58 , p 's < 0.0097) except for the dorsal attention network ($z = -0.47$, $p = 0.63$). In contrast, function predicted PMA better than structure for preterm infants. All but the dorsal and ventral attention networks from the functional connectome significantly predicted PMA in the preterm infant group. Only the limbic, default mode, and subcortical networks

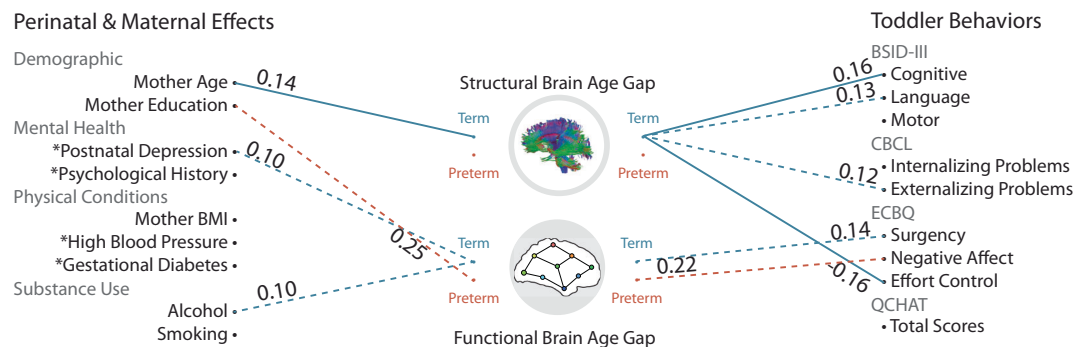


Fig. 4 | Brain age gaps (BAGs) were associated with maternal effects and toddler behaviors. Maternal mental health, physical health, demographics, and substance use correlate with BAGs for term and preterm infants, controlling for the infant's postmenstrual age. The BAGs also correlate with several later behaviors in toddlerhood, controlling for the infant's postmenstrual age. The p -values of two-sided Pearson's correlation are FDR-corrected. Dashed lines associations were not

significant after FDR correction, Solid lines associations were significant after FDR correction. BSID the Bayley Scales of Infant and Toddler Development, CBCL the Child Behavior Checklist, ECBQ the Early Childhood Behavior Questionnaire, Q-CHAT the Quantitative Checklist for Autism in Toddlers. Source data are provided as a Source Data file.

from the structural connectome predicted the PMA preterm infants. Models generated from a single network were numerically worse than the whole-brain models.

Structural and functional age for each network were correlated except for the dorsal attention network in term infants. Nevertheless, these correlations (r 's < 0.18) were smaller than at the whole-brain level ($r = 0.36$). For the three networks exhibiting significant age predictions for both structural and functional connectomes, significant correlations between structural and functional ages were observed for preterm infants (r 's > 0.25, p 's < 0.001). Structural and functional ages were more correlated in the preterm infants than in the term infants for the default mode ($z = -2.82$, $p = 0.0024$), the subcortical ($z = -3.1907$, $p = 0.00071$), but not the limbic networks ($z = -1.27$, $p = 0.10$).

Predictions using between-network connections are shown in Fig. S3. For structural connectomes, all between-network models, except for connections between the dorsal and ventral attention networks, predicted PMA for the term infants. For structural connectomes, between-network models predicted better (on average) than within-network models (between-network: mean $r = 0.54$; within-network: mean $r = 0.45$; $p = 0.046$, permutation testing, 1000 iterations). Like other analyses in term infants, between-networks models from structural connectomes performed better than models from functional connectomes. No differences in performance for within- and between-network models were observed for the functional connectomes. Similar trends were observed for models in preterm infants. Finally, we repeated PMA prediction based on individual lobes from structural connectomes. These results are shown in Fig. S4.

After calculating each network's structural and functional ages, we correlate the structural and functional ages between different canonical networks. A large correlation between the two networks' structural (or functional) age suggests that these networks have synchronous development. For term infants, structural ages were significantly correlated (r 's > 0.13, p 's < 0.05) across networks except for the structural ages from the dorsal attention and subcortical networks. As for functional ages, most were correlated across networks, except the functional ages from the frontoparietal and subcortical networks and the functional ages from the visual network to the other networks (Fig. 3c). Together, these results suggest that networks develop in synchrony in the term infant group. For preterm infants, all networks that predict PMA show strong correlations (r 's > 0.53, p 's < 0.001) in structural and functional ages between the different

networks (Fig. 3d). These correlations were generally stronger in preterm infants than in term infants.

Brain age gaps were associated with perinatal maternal exposures and toddler behaviors

Having established normative structural and functional ages, we asked how early exposures associated with individual deviations from the normative developmental trajectories. In other words, how do prenatal and early postnatal exposures associate with structure and functional BAGs? BAGs were defined as predicted postmenstrual age minus actual postmenstrual age. Sex and PMA were regressed from the BAGs to adjust for the mean bias in the brain age prediction³⁵. BAGs greater than 0 indicate that the predicted brain age is greater than the actual age. BAGs less than 0 indicate the opposite. Maternal information was collected after birth. We studied ten prenatal and early postnatal measures across four common exposure types: maternal mental health (postnatal depression, lifetime psychiatry history), maternal physical health (BMI, high blood pressure, gestational diabetes), maternal demographics (age, education), and maternal substance use (smoking, alcohol).

We further investigated if BAGs after birth exhibit a long-term influence on toddler behaviors. Cognitive and behavioral assessments were performed at 18 months. These assessments included the Bayley Scales of Infant and Toddler Development (BSID)³⁶, the Child Behavior Checklist (CBCL)³⁷, the Early Childhood Behavior Questionnaire (ECBQ)³⁸, and the Quantitative Checklist for Autism in Toddlers (Q-CHAT)³⁹. Correlations between the perinatal exposures and toddler outcomes are shown in Tables S6–8.

Linear models were used to associate BAGs and exposures/behaviors (Fig. 4). For the term group, maternal age positively correlated with structural BAGs ($r = 0.14$, $p = 0.0042$, $pFDR = 0.048$). Associations with alcohol use, postnatal depression, and gestational diabetes did not survive FDR correction. For term infants, structural BAGs positively correlated with BSID cognitive ($r = 0.16$, $p = 0.0036$, $pFDR = 0.020$) but negatively correlated with ECBQ effort control ($r = -0.16$, $p = 0.0040$, $pFDR = 0.020$). Associations with BSID language, CBCL externalizing problems, ECBQ surgency, and ECBQ negative affect did not survive FDR correction. In exploratory analyses, we found that structural BAGs at birth partially mediated the association between maternal age and externalizing problems at 18 months old in the term group (average direct effect = -0.10 , $p < e-16$; Total effect = -0.086 , $p = 0.002$; Prop. mediated = -0.14 , $p = 0.030$).

We repeated these analyses with BAGs from the SVR models. For the significant associations reported above, maternal age positively correlated with structural BAGs for term infants ($r=0.10$, $p=0.030$, $pFDR=0.20$). Structural BAGs positively correlated with BSID cognitive ($r=0.13$, $p=0.013$, $pFDR=0.13$) but negatively correlated with ECBQ effort control ($r=-0.004$, $p=0.95$, $pFDR=0.95$) for term infants. Overall, results from CPM and SVR models show consistency, with significant correlations between association results from CPM and those from SVR (Tables S3 and S4).

Figure S5 shows association analyses with other covariates regressed. We also included the prediction results of perinatal maternal exposure and toddler behaviors using infants' structural and functional connectomes in Fig. S6. Associations between gestational/postmenstrual ages, perinatal exposures, and toddler outcomes are shown in Fig. S7.

Discussion

Using normative modeling, we establish that structural and functional connectomes accurately predict postmenstrual ages in term and preterm infants scanned within the first months of life. We observed greater predictive accuracy of structural connectomes compared to functional connectomes. Further, predicted structural and functional age were correlated. Preterm infants exhibited a greater correlation between structural and functional ages and weaker prediction from structural connectomes than term infants. At the network level, nearly all canonical brain networks—even putatively later developing ones—accurately predict PMA. In term infants, BAGs correlated with several early life exposures and toddler cognition. These findings highlight the value of normative structural and functional development models in the perinatal period, where deviations from the normative trajectory are associated with early-life maternal exposures and later behavior.

The structural connectome develops before the functional connectome⁴. That structural connectomes consistently predicted PMA more accurately than functional connectomes for term infants aligns with this literature. Structural connectome is highly organized at birth with adult-like hubs and modules². These richer features provide more information for the machine learning algorithms to learn from and increase prediction performance. Interestingly, between-network connections predicted PMA better than within-network connections, consistent with the rapid development of cross-hemisphere connections during this period⁴⁰. The frontal lobe was the best predicting lobe for structural connectivity. Several core behaviors for infants are located in the frontal lobe. For example, morphometric features and structural connectivity in language regions (i.e., Broca's region) are reportedly primed to learn language from birth^{41,42}. The functional connectivity associated with these regions may take years to form^{8,43–45}.

Nevertheless, PMA predictions with functional connectomes were highly accurate, with an average error of only 2.5 days worse than the structural connectomes. These results are consistent with recent research showing strong PMA prediction with functional connectomes in young infants⁹. In term infants, all networks predicted PMA (except ventral attention). Critically, there were no differences between higher-order networks that develop more slowly (e.g., DMN or FPN)⁷ and lower-order networks (e.g., motor or visual) that develop earlier^{46,47}. Indeed, the FPN exhibited the greatest predictive accuracy. These results suggest that networks like the DMN or FPN might exhibit richer individual differences during the first postnatal month than previously thought. Additionally, the moderate correlation between structural and functional ages suggests a dependency between structural and functional development. Presumably, structural maturation serves as the foundation for later functional development. However, this causality cannot be inferred from our current results.

Preterm infants exhibited several different patterns in brain age compared to term infants. They had a higher correlation between structural and functional age and between structural and functional

BAGs. In addition, structural connections at the individual network level were less predictive, while functional connections were more predictive in preterm than term infants. Preterm birth accelerates functional trajectories due to earlier exposure to a postnatal environment⁴⁸. This observation may explain the differences between term and preterm infants, such as the increased prediction accuracy from functional connectomes. Alternatively, preterm infants exhibit altered structural connectivity^{49,50}—which, in turn, may be driving reduced prediction accuracy of the structural connectomes. A combination of altered structural and functional neurodevelopment is most likely responsible for these differences.

Early life exposures associate with brain age. Exposure to maternal distress (e.g., stress, depression, and anxiety) and substance use are commonly studied. Rather than focusing on brain regions of interest, such as the hippocampus and amygdala^{51,52}, as in most works, our findings exhibit that altered connectivity extends beyond these regions and to the whole brain level. We also find altered structural and functional development for less commonly studied exposures like gestational diabetes and maternal age. These maternal effects have distinct implications for term and preterm infants. One possible reason could be the differences in the critical windows during which maternal effects influence them. For example, maternal age is associated with increased BAGs in term, but not preterm infants. Both young and advanced maternal ages are risk factors for preterm birth, which may explain differences in associations with maternal age for term and preterm infants^{53–55}. Moreover, the biological pathways from exposures to altered brain development might cause differences. Likely, multiple biological systems, including the maternal immune system and hypothalamic-pituitary-adrenal axis, are candidate pathways⁵⁶. Many exposures activate inflammatory cytokines and proteins, which can then cross the placenta. It is hypothesized that while inflammatory cytokines contribute to fetal brain development, inappropriately high levels may alter cellular survival, proliferation, differentiation, axonal growth, and synaptogenesis^{57,58}.

A hope for infant neuroimaging studies is to predict the risk for poor developmental outcomes in toddlerhood or later^{59,60}. We found that BAGs are associated with several toddler outcomes. Importantly, these associations were not only in a single direction. In other words, positive and negative BAGs could be both associated with worse outcomes. For example, a negative BAG is associated with worse cognition, while a positive one is associated with worse self-regulation. A large deviation from one's peers, regardless of direction, may be equally negative from infancy to adolescence⁶¹. This explanation aligns with the theory of critical periods in development. These periods are developmental windows where the brain is the most plastic to learning a skill or behavior. Changing the brain and the behavior it subserves outside this window is more difficult^{62,63}. A normative range for BAGs could be used to define if an individual is missing a critical period. For example, a large BAG in either direction could suggest an infant is outside a critical period, resulting in worse developmental outcomes. However, longitudinal BAGs likely are needed to map when an individual enters and exits these critical periods and if they are indeed missed.

Our work has several strengths, including a large sample of infants with high-quality neuroimaging data, multimodal normative modeling, and longitudinal follow-up data in toddlerhood. However, several limitations should be acknowledged. First, while our study includes longitudinal data (prenatal exposures, postnatal MRI, and toddler behavior), measures were sparsely collected. Given the rapid change from infancy to toddlerhood, dense sampling is needed to account for the numerous interacting pre- and postnatal influences and establish direct relationships between prenatal exposures, brain development, and cognitive outcomes. It will also facilitate identifying critical periods of vulnerability and possible intervention. Second, Even though our current sample size is large for infant neuroimaging studies in preterms, preterm birth is highly heterogeneous in its causes and outcomes⁶⁴.

Therefore, this size and variability in preterm birth effects might not represent the larger population of preterm infants. Third, the absence of genetic analysis in the current study might overlook the interplay between genetic factors and early life exposures on neurodevelopment. Genetic variations help shape individual differences in functional^{65–67} and structural connectivity^{68–70}. These variations further interact with the environmental effects (i.e., epigenetics/maternal)^{71–73}. Integrating genetic data into future studies could further nuance our results. Finally, the reliance on maternal self-report measures and lack of detailed medical records may introduce bias and measurement errors. For example, we lack details about the frequency of tobacco and alcohol use and the actual blood pressure measurements. Replication of each early life exposure with detailed measurements during pregnancy is required.

In conclusion, we established normative models of structural and functional aging during the perinatal period. Results highlight the complex interplay between an infant's brain age, early life exposures, and later cognitive behaviors. Overall, brain age and BAGs provide a valuable tool for studying neurodevelopment in infants.

Methods

Participants

All data were obtained from the Developing Human Connectome Project³¹ (dHCP, <http://www.developingconnectome.org/>), a longitudinal study of infant brain development with open access. The study received approval from the National Research Ethics Service West London committee. Participating families provided written consent before imaging. Our sample included 437 term infants (203 female, 234 male) and 174 preterm infants (74 female, 100 male) from the second data release of dHCP. Preterm infants were born between 23.00 and 36.86 weeks of gestation and scanned between 26.71 and 45.14 weeks. A subset of preterm infants were retested ($n = 73$) at the term-equivalent ages, between 38.43 and 44.86 weeks. Term infants were born between 37.00 and 42.29 weeks of gestation and scanned between 37.43 and 44.71 weeks. Demographic information about the infants is presented in Table 1. More information, such as the primary clinical reason for the episode of care and the mother's ethnicity, were summarized in Tables S9 and S10.

MRI acquisition

All images were collected in the Evelina Newborn Imaging Center, St Thomas' Hospital, London, UK. MRI data were acquired with a Philips Achieva 3 T scanner (Philips Medical Systems, Best, The Netherlands) with a dHCP-customized neonatal imaging system, including a 32-channel receive neonatal head coil (Rapid Biomedical GmbH, Rimplar, DE)³¹. Infants were scanned during unsedated sleep after feeding and immobilization in a vacuum-evacuated bag, with hearing protection and physiological monitoring (including pulse oximetry, body temperature, and electrocardiography data) applied during scanning.

T2-weighted images were obtained using a Turbo spin echo sequence (TR = 12 s, TE = 156 ms, SENSE factor 2.11 (axial) and 2.54 (sagittal)) with overlapping slices (resolution = $0.8 \times 0.8 \times 1.6 \text{ mm}^3$). T2w images were motion-corrected and super-resolved to a resolution of $0.8 \times 0.8 \times 0.8 \text{ mm}^3$ ⁷⁴. Diffusion-weighted imaging (DWI) was obtained in 300 directions (TR = 3.8 s, TE = 90 ms, SENSE factor 1.2, multiband factor 4, and resolution $1.5 \times 1.5 \times 3 \text{ mm}^3$ with 1.5 mm slice overlap) with b-values of 400 s/mm², 1000 s/mm² and 2600 s/mm² spherically distributed in 64, 88 and 128 directions respectively using interleaved phase encoding⁷⁵. BOLD fMRI runs were 15 minutes 3 seconds (2300 time volumes) and used a multislice gradient-echo planar imaging (EPI) sequence with TR 0.392 s, TE 0.038 s, flip angle 34 degrees, and acquired spatial resolution 2.15 mm isotropic⁷⁶.

Structural connectome processing

Diffusion MRI was reconstructed at an in-plane resolution of 1.5 mm and slice thickness of 1.5 mm. Images were denoised and corrected for

motion, eddy current, Gibbs ringing, and susceptibility artifact with the diffusion SHARD pipeline. In-scanner head motion was estimated by the SHARD outlier ratio, which is the mean outlier weight of all slices detected in slice-to-volume reconstruction. A quality check was conducted by neighboring DWI correction (NDC)⁷⁷, leading to 34 scans being excluded due to their low NDC values calculated by median value-based outlier detection. The accuracy of b-table orientation was examined by comparing fiber orientations with those of a population-averaged template. Then, the reconstruction of the diffusion data was performed in native space with generalized q-sampling imaging (GQI)⁷⁸ with a diffusion sampling length ratio of 1.25. The tensor metrics were calculated and analyzed using the resource allocation (TG-CIS200026) at Extreme Science and Engineering Discovery Environment (XSEDE) resources⁷⁹.

After reconstructing images with GQI, the whole-brain fiber tracking was conducted with DSI-studio (<http://dsi-studio.labsolver.org/>) with quantitative anisotropy (QA) as the termination threshold. QA values were computed in each voxel in their native space for every subject. The tracking parameters were set as the angular cutoff of 60 degrees, step size of 1.0 mm, minimum length of 30 mm, and maximum length of 300 mm. The whole-brain fiber tracking process was performed with the FACT algorithm until 1,000,000 streamlines were reconstructed for each individual. Here, we used a neonatal AAL-aligned brain parcellation with 90 nodes⁸⁰ to construct the structural connectome for each infant. T2-weighted images in native DWI space were used to provide information on region segmentation during the construction of connectomes. The structural connectome for each individual was then constructed with a connectivity threshold of 0.001. The pairwise connectivity strength was calculated as the average QA value of each fiber connecting the two end regions. This resulted in a 90x90 adjacent matrix for each individual as the brain structural connectome matrix.

Functional connectome processing

fMRI data was preprocessed with the dHCP functional pipeline⁸¹, including echo distortion correction, motion correction, independent component analysis (ICA) denoising, and registered to individual T2w native space. All subsequent preprocessing was performed with Bio-Image Suite (<https://bioimagesuiteweb.github.io/webapp/>). Mean time courses were regressed in white matter, cerebrospinal fluid, and gray matter. The neonatal AAL-aligned brain parcellation with 90 nodes was applied to the preprocessed fMRI data. Mean time courses of each node pair were correlated, and correlation coefficients were Fisher transformed, generating one 90x90 resting-state functional connectivity matrix per individual.

Brain age

Predictive models of an infant's PMA were built with connectome-based predictive modeling (CPM) using structural and functional connectomes⁸². Predictive models were trained for term and preterm infant groups separately. For each model, the feature was selected from structural or functional connectomes and threshold at $p = 0.05$, with sex, brain volume, and head motion controlled. 10-fold cross-validation was performed. The infants were randomly divided into ten subgroups, among which nine subgroups were used as training and one subgroup as a testing group. Model training involves feature selection of relative brain features within the training group using Pearson's correlation. The brain features (e.g., edge strength in a connectome) significantly correlated ($p < 0.05$) with the post-menstrual ages were retained and separated into a positive network (i.e., edges positively associated with PMA) and a negative network (i.e., edges negatively associated with PMA). Next, the selected features for each individual were summed into a single number. Linear regression was then used to model this summary score and the phenotype in the training group. Finally, this model was applied to the testing group. This process was repeated iteratively, with each subgroup being the testing group once, generating a predicted result for

Table 2 | Maternal characteristics

| | <i>n</i> | mean (std) |
|---------------------------------------|---------------------------------------|--------------|
| Age at expected delivery | 611 | 33.80 (5.03) |
| Pre-pregnancy body mass index | 600 | 24.45 (4.60) |
| Last age in continuous education | 437 | 23.40 (4.99) |
| *Preeclampsia or eclampsia | 51/608 | |
| *Gestational diabetes | 37/611 | |
| *Psychological history | 79/600 | |
| Postnatal depression | 535 | 5.51 (4.34) |
| Substance use during perinatal period | alcohol(number of units per week) | 45/606 |
| | smoking(number of cigarettes per day) | 19/606 |

each individual in the dataset. We repeated each prediction process 100 times and averaged the predicted results as the brain ages. Brain age gap (BAG) was determined by subtracting the actual post-menstrual age from the predicted postmenstrual age, serving as an indicator of whether the predicted brain age appears older (age gap > 0) or younger (age gap < 0) than their actual ages. Sex and PMA were regressed from the BAGs to adjust for the mean bias in the brain age prediction. Analyses with other covariates regressed were shown in the supplementary information.

To calculate network ages, connectomes were separated into eight canonical functional networks³⁴: visual, somatomotor, frontoparietal, default mode, dorsal attention, ventral attention, limbic, and subcortical networks (see Table S5). For each network, the predicted PMA was generated based only on the connections within this network using the same CPM procedure described above. Similarly, we predict PMA using only the connections between two canonical networks. For validation purposes, we repeated the prediction process with support vector machines, and results were provided in supplementary information Tables S1–4.

Perinatal exposures

The influence of several perinatal exposures on infant brain development was investigated, as summarized in Tables 2 and S11. Maternal physical health included body mass index (BMI), the occurrence of high blood pressure (i.e., pre-eclampsia, Hemolysis, Elevated Liver enzymes, and Low Platelets, or pregnancy-induced hypertension), and gestational diabetes. Maternal mental health included postnatal depression screened by the Edinburgh Postnatal Depression Scale (EPDS)⁸³ and maternal history of mental health problems. Maternal substance use included the use of alcohol and tobacco during pregnancy. Maternal demographics included maternal age at expected delivery and education level. For the continuous measures (maternal age, BMI, EPDS level, alcohol, and smoking use level), Pearson’s correlations were used to quantify the association between the measures and infant brain age gaps. For the binary measures (psychological history, high blood pressure, gestational diabetes, and the use of recreational drugs), two-sample t-tests were used to test the effect on infant brains. The t-statistics were then transformed into r-values for comparison across measures. All p-values were corrected for multiple comparisons with the Benjamini–Hochberg false discovery rate (FDR) method.

Toddler outcomes

Four commonly-used behavioral measures were collected during the follow-up visits at 18 months (Table 1). Bayley Scales Of Infant and Toddler Development Third Version (BSID-III)³⁶ evaluates three areas of development: cognitive, language, and motor. Child Behavior Checklist (CBCL)³⁷ assesses the child’s psychological risks in internalizing problems, summing the anxious/depressed, withdrawn-depressed, and somatic complaints scores, and externalizing problems, including rule-breaking and aggressive behaviors. The Early

Childhood Behavior Questionnaire (ECBQ) measures a toddler’s emotional and behavioral regulation skills through parents’ reports³⁸. Quantitative Checklist for Autism in Toddlers (Q-CHAT) evaluates the risk in the social-emotional performance during toddlerhood³⁹. Pearson’s correlations between these measures and BAGs were calculated. All p-values were corrected for multiple comparisons with the Benjamini–Hochberg false discovery rate (FDR) method.

Reporting summary

Further information on research design is available in the Nature Portfolio Reporting Summary linked to this article.

Data availability

Raw Data from the Developing Human Connectome Project is publicly available at <http://www.developingconnectome.org/data-release/third-data-release> and can be downloaded upon request from NDA. Source data are provided with this paper.

Code availability

Preprocessing code can be found at https://brain.labsolver.org/hcp_d2.html for brain structural connectome and <https://medicine.yale.edu/bioimaging/suite/> for brain functional connectome. Custom analysis code is available at https://github.com/huiliiii/infant_brain_age.

References

- Geng, X. et al. Structural and maturational covariance in early childhood brain development. *Cereb. Cortex* **27**, 1795–1807 (2017).
- Ball, G. et al. Rich-club organization of the newborn human brain. *Proc. Natl. Acad. Sci. USA* **111**, 7456–7461 (2014).
- Sun, H. et al. Network controllability of structural connectomes in the neonatal brain. *Nat. Commun.* **14**, 5820 (2023).
- Ciarrusta, J. et al. The developing brain structural and functional connectome fingerprint. *Dev. Cogn. Neurosci.* **55**, 101117 (2022).
- Gilmore, J. H., Knickmeyer, R. C. & Gao, W. Imaging structural and functional brain development in early childhood. *Nat. Rev. Neurosci.* **19**, 123–137 (2018).
- Heuvel, M. Ivanden & Thomason, M. E. Functional connectivity of the human brain in utero. *Trends Cogn. Sci.* **20**, 931–939 (2016).
- Gao, W. et al. Functional network development during the first year: relative sequence and socioeconomic correlations. *Cereb. Cortex* **25**, 2919–2928 (2015).
- Scheinost, D. et al. Functional connectivity for the language network in the developing brain: 30 weeks of gestation to 30 months of age. *Cereb. Cortex* **32**, 3289–3301 (2022).
- Nielsen, A. N. et al. Maturation of large-scale brain systems over the first month of life. *Cerebral Cortex* bhac242 <https://doi.org/10.1093/cercor/bhac242> (2022).
- Yin, C. et al. Anatomically interpretable deep learning of brain age captures domain-specific cognitive impairment. *Proc. Natl. Acad. Sci. USA* **120**, e2214634120 (2023).

11. More, S. et al. Brain-age prediction: a systematic comparison of machine learning workflows. *NeuroImage* **270**, 119947 (2023).
12. Kaufmann, T. et al. Common brain disorders are associated with heritable patterns of apparent aging of the brain. *Nat. Neurosci.* **22**, 1617–1623 (2019).
13. Cole, J. H. et al. Brain age predicts mortality. *Mol. Psychiatry* **23**, 1385–1392 (2018).
14. Kardan, O. et al. Resting-state functional connectivity identifies individuals and predicts age in 8-to-26-month-olds. *Dev. Cogn. Neurosci.* **56**, 101123 (2022).
15. Smyser, C. D. et al. Prediction of brain maturity in infants using machine-learning algorithms. *NeuroImage* **136**, 1–9 (2016).
16. Li, Y. et al. Brain connectivity based graph convolutional networks and its application to infant age prediction. *IEEE Trans. Med. Imaging* **41**, 2764–2776 (2022).
17. Taoudi-Benchekroun, Y. et al. Predicting age and clinical risk from the neonatal connectome. *NeuroImage* **257**, 119319 (2022).
18. Kawahara, J. et al. BrainNetCNN: convolutional neural networks for brain networks; towards predicting neurodevelopment. *NeuroImage* **146**, 1038–1049 (2017).
19. Fenchel, D. et al. Development of microstructural and morphological cortical profiles in the neonatal brain. *Cereb. Cortex* **30**, 5767–5779 (2020).
20. Brown, C. J. et al. Prediction of brain network age and factors of delayed maturation in very preterm infants. In *Medical Image Computing and Computer Assisted Intervention–MICCAI 2017* (eds Descoteaux, M. et al.) 84–91 (Springer International Publishing, https://doi.org/10.1007/978-3-319-66182-7_10 2017).
21. Galdi, P. et al. Neonatal morphometric similarity mapping for predicting brain age and characterizing neuroanatomic variation associated with preterm birth. *NeuroImage Clin.* **25**, 102195 (2020).
22. Kumpulainen, V. et al. Prenatal and postnatal maternal depressive symptoms are associated with white matter integrity in 5-year-olds in a sex-specific manner. *Biol. Psychiatry* **94**, 924–935 (2023).
23. Qiu, A. et al. Maternal positive mental health during pregnancy impacts the hippocampus and functional brain networks in children. *Nat. Mental Health* 1–8 <https://doi.org/10.1038/s44220-024-00202-8> (2024).
24. Lugo-Candelas, C. et al. Maternal mental health and offspring brain development: an umbrella review of prenatal interventions. *Biol. Psychiatry* **93**, 934–941 (2023).
25. Rifkin-Graboi, A. et al. Antenatal maternal anxiety predicts variations in neural structures implicated in anxiety disorders in newborns. *J. Am. Acad. Child Adolesc. Psychiatry* **54**, 313–321.e2 (2015).
26. Gale-Grant, O. et al. Parental age effects on neonatal white matter development. *NeuroImage: Clin.* **27**, 102283 (2020).
27. KC, K., Shakya, S. & Zhang, H. Gestational diabetes mellitus and macrosomia: a literature review. *Ann. Nutr. Metab.* **66**, 14–20 (2015).
28. Magee, L. A. et al. Less-tight versus tight control of hypertension in pregnancy. *N. Engl. J. Med.* **372**, 407–417 (2015).
29. Rompala, G., Nomura, Y. & Hurd, Y. L. Maternal cannabis use is associated with suppression of immune gene networks in placenta and increased anxiety phenotypes in offspring. *Proc. Natl. Acad. Sci. USA* **118**, e2106115118 (2021).
30. Ross, E. J., Graham, D. L., Money, K. M. & Stanwood, G. D. Developmental consequences of fetal exposure to drugs: what we know and what we still must learn. *Neuropsychopharmacol.* **40**, 61–87 (2015).
31. Hughes, E. J. et al. A dedicated neonatal brain imaging system. *Magn. Reson. Med.* **78**, 794–804 (2017).
32. De Asis-Cruz, J. et al. Functional brain connectivity in ex utero premature infants compared to in utero fetuses. *NeuroImage* **219**, 117043 (2020).
33. Inder, T. E. et al. Neuroimaging of the preterm brain: review and recommendations. *J. Pediatr.* **237**, 276–287.e4 (2021).
34. Thomas Yeo, B. T. et al. The organization of the human cerebral cortex estimated by intrinsic functional connectivity. *J. Neurophysiol.* **106**, 1125–1165 (2011).
35. Smith, S. M., Vidaurre, D., Alfaro-Almagro, F., Nichols, T. E. & Miller, K. L. Estimation of brain age delta from brain imaging. *NeuroImage* **200**, 528–539 (2019).
36. Bayley, N. *Bayley Scales of Infant and Toddler Development*, 3rd edn. <https://doi.org/10.1037/t14978-000> (2005).
37. Mazefsky, C. A., Anderson, R., Conner, C. M. & Minshew, N. Child behavior checklist scores for school-aged children with autism: preliminary evidence of patterns suggesting the need for referral. *J. Psychopathol. Behav. Assess.* **33**, 31–37 (2011).
38. Putnam, S. P., Gartstein, M. A. & Rothbart, M. K. Measurement of fine-grained aspects of toddler temperament: the early childhood behavior questionnaire. *Infant Behav. Dev.* **29**, 386–401 (2006).
39. Allison, C. et al. The Q-CHAT (Quantitative CHecklist for Autism in Toddlers): a normally distributed quantitative measure of autistic traits at 18–24 months of age: preliminary report. *J. Autism Dev. Disord.* **38**, 1414–1425 (2008).
40. Thomason, M. E. et al. Cross-hemispheric functional connectivity in the human fetal brain. *Sci. Transl. Med.* **5**, 173ra24 (2013).
41. Brauer, J., Anwender, A., Perani, D. & Friederici, A. D. Dorsal and ventral pathways in language development. *Brain Lang.* **127**, 289–295 (2013).
42. WITELSON, S. F. & PALLIE, W. Left hemisphere specialization for language in the newborn: neuroanatomical evidence of asymmetry. *Brain* **96**, 641–646 (1973).
43. Emerson, R. W., Gao, W. & Lin, W. Longitudinal study of the emerging functional connectivity asymmetry of primary language regions during infancy. *J. Neurosci.* **36**, 10883–10892 (2016).
44. Perani, D. et al. Neural language networks at birth. *Proc. Natl. Acad. Sci. USA* **108**, 16056–16061 (2011).
45. Bruchhage, M. M. K., Ngo, G.-C., Schneider, N., D'Sa, V. & Deoni, S. C. L. Functional connectivity correlates of infant and early childhood cognitive development. *Brain Struct. Funct.* **225**, 669–681 (2020).
46. Allievi, A. G. et al. Maturation of sensori-motor functional responses in the preterm brain. *Cereb. Cortex* **26**, 402–413 (2016).
47. Dehaene-Lambertz, G., Dehaene, S. & Hertz-Pannier, L. Functional neuroimaging of speech perception in infants. *Science* **298**, 2013–2015 (2002).
48. Doria, V. et al. Emergence of resting state networks in the preterm human brain. *Proc. Natl. Acad. Sci. USA* **107**, 20015–20020 (2010).
49. Ball, G. et al. Development of cortical microstructure in the preterm human brain. *Proc. Natl. Acad. Sci. USA* **110**, 9541–9546 (2013).
50. Brenner, R. G., Wheelock, M. D., Neil, J. J. & Smyser, C. D. Structural and functional connectivity in premature neonates. *Semin. Perinatol.* **45**, 151473 (2021).
51. Buss, C. et al. Maternal cortisol over the course of pregnancy and subsequent child amygdala and hippocampus volumes and affective problems. *Proc. Natl. Acad. Sci. USA* **109**, E1312–E1319 (2012).
52. Qiu, A. et al. Maternal anxiety and infants' hippocampal development: timing matters. *Transl. Psychiatry* **3**, e306–e306 (2013).
53. Fuchs, F., Monet, B., Ducruet, T., Chaillet, N. & Audibert, F. Effect of maternal age on the risk of preterm birth: a large cohort study. *PLoS One* **13**, e0191002 (2018).
54. Waldenström, U., Cnattingius, S., Vixner, L. & Norman, M. Advanced maternal age increases the risk of very preterm birth, irrespective of parity: a population-based register study. *BJOG Int. J. Obstet. Gynaecol.* **124**, 1235–1244 (2017).
55. Da Silva, A. A. M. et al. Young maternal age and preterm birth. *Paediatr. Perinat. Epidemiol.* **17**, 332–339 (2003).
56. Monk, C., Lugo-Candelas, C. & Trumpff, C. Prenatal developmental origins of future psychopathology: mechanisms and pathways. *Annu. Rev. Clin. Psychol.* **15**, 317–344 (2019).

57. Mehler, M. F. & Kessler, J. A. Hematolymphopoietic and inflammatory cytokines in neural development. *Trends Neurosci.* **20**, 357–365 (1997).
58. Deverman, B. E. & Patterson, P. H. Cytokines and CNS development. *Neuron* **64**, 61–78 (2009).
59. Scheinost, D. et al. Machine learning and prediction in fetal, infant, and toddler neuroimaging: a review and primer. *Biol. Psychiatry* **93**, 893–904 (2023).
60. Luby, J. L. et al. Basic environmental supports for positive brain and cognitive development in the first year of life. *JAMA Pediatr.* <https://doi.org/10.1001/jamapediatrics.2024.0143> (2024).
61. Beck, D. et al. Dimensions of early life adversity are differentially associated with patterns of delayed and accelerated brain maturation. *Biol. Psychiatry* <https://doi.org/10.1016/j.biopsych.2024.07.019> (2024).
62. Margolis, E. T. & Gabard-Durnam, L. J. Prenatal influences on postnatal neuroplasticity: Integrating DOHaD and sensitive/critical period frameworks to understand biological embedding in early development. *Infancy* (2024).
63. Nelson, C. A. & Gabard-Durnam, L. J. Early adversity and critical periods: neurodevelopmental consequences of violating the expectable environment. *Trends Neurosci.* **43**, 133–143 (2020).
64. Romero, R., Dey, S. K. & Fisher, S. J. Preterm labor: one syndrome, many causes. *Science* **345**, 760–765 (2014).
65. Gao, W., Lin, W., Grewen, K. & Gilmore, J. H. Functional connectivity of the infant human brain: plastic and modifiable. *Neuroscientist* **23**, 169–184 (2017).
66. Blanchett, R. et al. Genetic and environmental factors influencing neonatal resting-state functional connectivity. *Cereb. Cortex* **33**, 4829–4843 (2023).
67. Stoeklein, S. et al. Variable functional connectivity architecture of the preterm human brain: Impact of developmental cortical expansion and maturation. *Proc. Natl. Acad. Sci. USA* **117**, 1201–1206 (2020).
68. Knickmeyer, R. C. et al. Common variants in psychiatric risk genes predict brain structure at birth. *Cereb. Cortex* **24**, 1230–1246 (2014).
69. Krishnan, M. L. et al. Machine learning shows association between genetic variability in PPARG and cerebral connectivity in preterm infants. *Proc. Natl. Acad. Sci. USA* **114**, 13744–13749 (2017).
70. Alex, A. M. et al. Genetic influences on the developing young brain and risk for neuropsychiatric disorders. *Biol. Psychiatry* **93**, 905–920 (2023).
71. Sparrow, S. et al. Epigenomic profiling of preterm infants reveals DNA methylation differences at sites associated with neural function. *Transl. Psychiatry* **6**, e716–e716 (2016).
72. Fumagalli, M. et al. From early stress to 12-month development in very preterm infants: preliminary findings on epigenetic mechanisms and brain growth. *PLoS One* **13**, e0190602 (2018).
73. Qiu, A. et al. COMT haplotypes modulate associations of antenatal maternal anxiety and neonatal cortical morphology. *AJP* **172**, 163–172 (2015).
74. Cordero-Grande, L., Hughes, E. J., Hutter, J., Price, A. N. & Hajnal, J. V. Three-dimensional motion corrected sensitivity encoding reconstruction for multi-shot multi-slice MRI: application to neonatal brain imaging. *Magn. Reson. Med.* **79**, 1365–1376 (2018).
75. Scheid, B. H. et al. Time-evolving controllability of effective connectivity networks during seizure progression. *Proc. Natl. Acad. Sci. USA* **118**, e2006436118 (2021).
76. Price, A. N. et al. Accelerated Neonatal fMRI using Multiband EPI. *Proc. Int. Soc. Mag. Reson. Med.* **23**, 3911 (2015).
77. Yeh, F.-C. et al. Differential tractography as a track-based biomarker for neuronal injury. *NeuroImage* **202**, 116131 (2019).
78. Yeh, F.-C., Wedeen, V. J. & Tseng, W.-Y. I. Generalized q -sampling Imaging. *IEEE Trans. Med. Imaging* **29**, 1626–1635 (2010).
79. Towns, J. et al. XSEDE: accelerating scientific discovery. *Comput. Sci. Eng.* **16**, 62–74 (2014).
80. Shi, F. et al. Infant brain atlases from neonates to 1- and 2-year-olds. *PLoS One* **6**, e18746 (2011).
81. Fitzgibbon, S. P. et al. The developing Human Connectome Project (dHCP) automated resting-state functional processing framework for newborn infants. *NeuroImage* **223**, 117303 (2020).
82. Shen, X. et al. Using connectome-based predictive modeling to predict individual behavior from brain connectivity. *Nat. Protoc.* **12**, 506–518 (2017).
83. Matthey, S., Barnett, B. & White, T. The Edinburgh postnatal depression scale. *Br. J. Psychiatry* **182**, 368–368 (2003).

Acknowledgements

This study was supported by the Wellcome Leap 1kD Program (obtained by D.S.) and NIMH (R01 MH126133 to D.S. and M.N.S.; K24 MH127381 to M.N.S.) Data were provided by the developing Human Connectome Project, KCL-Imperial-Oxford Consortium funded by the European Research Council under the European Union Seventh Framework Program (FP/2007-2013)/ERC Grant Agreement no. [319456]. We are grateful to the families who generously supported this trial.

Author contributions

H.S.: conceptualization, methodology, investigation, result visualization, and writing-original draft. S.M., M.K., and X.H.: methodology, writing-review and editing; B.C. and M.N.S.: writing-review and editing; D.S.: conceptualization, supervision and writing-review and editing.

Competing interests

The authors declare no competing interests.

Additional information

Supplementary information The online version contains supplementary material available at <https://doi.org/10.1038/s41467-024-54657-5>.

Correspondence and requests for materials should be addressed to Huili Sun.

Peer review information *Nature Communications* thanks Paola Galdi and the other, anonymous, reviewer(s) for their contribution to the peer review of this work. A peer review file is available.

Reprints and permissions information is available at <http://www.nature.com/reprints>

Publisher's note Springer Nature remains neutral with regard to jurisdictional claims in published maps and institutional affiliations.

Open Access This article is licensed under a Creative Commons Attribution-NonCommercial-NoDerivatives 4.0 International License, which permits any non-commercial use, sharing, distribution and reproduction in any medium or format, as long as you give appropriate credit to the original author(s) and the source, provide a link to the Creative Commons licence, and indicate if you modified the licensed material. You do not have permission under this licence to share adapted material derived from this article or parts of it. The images or other third party material in this article are included in the article's Creative Commons licence, unless indicated otherwise in a credit line to the material. If material is not included in the article's Creative Commons licence and your intended use is not permitted by statutory regulation or exceeds the permitted use, you will need to obtain permission directly from the copyright holder. To view a copy of this licence, visit <http://creativecommons.org/licenses/by-nc-nd/4.0/>.

© The Author(s) 2024